

# Diamond and diamond-like carbon MEMS

J K Luo<sup>1,4</sup>, Y Q Fu<sup>1</sup>, H R Le<sup>2</sup>, J A Williams<sup>1</sup>, S M Spearing<sup>3</sup>  
and W I Milne<sup>1</sup>

<sup>1</sup> Department of Engineering, Cambridge University, 9 JJ Thomson Avenue, Cambridge, CB3 0FA, UK

<sup>2</sup> Division of Mechanical Engineering & Mechatronics, University of Dundee, Dundee, DD1 4HN, UK

<sup>3</sup> School of Engineering Science, University of Southampton, Southampton, SO17 1QJ, UK

<sup>4</sup> Centre for Material Research and Innovation, Bolton University, Bolton, BL3 5AB, UK

Received 21 December 2006, in final form 12 February 2007

Published 28 June 2007

Online at [stacks.iop.org/JMM/17/S147](http://stacks.iop.org/JMM/17/S147)

## Abstract

Diamond and diamond-like carbon (DLC) thin films possess a number of unique and attractive material properties that are unattainable from Si and other materials. These include high values of Young's modulus, hardness, tensile strength and high thermal conductivity, low thermal expansion coefficient combined with low coefficients of friction and good wear resistance. As a consequence, they are finding increasing applications in micro-electro-mechanical systems (MEMS). This paper reviews these distinctive material properties from an engineering design point of view and highlights the applications of diamond and DLC materials in various MEMS devices. Applications of diamond and DLC films in MEMS are in two categories: surface coatings and structural materials. Thin diamond and DLC layers have been used as coatings mainly to improve the wear and friction of micro-components and to reduce stiction between microstructures and their substrates. The high values of the elastic modulus of diamond and DLC have been exploited in the design of high frequency resonators and comb-drives for communication and sensing applications. Chemically modified surfaces and structures of diamond and DLC films have both been utilized as sensor materials for sensing traces of gases, to detect bio-molecules for biological research and disease diagnosis.

(Some figures in this article are in colour only in the electronic version)

## 1. Introduction

Micro-electro-mechanical systems (MEMS or microsystems) encompass technologies implemented at characteristic lengths from nanometres to microns. This emerging technology offers environmentally friendly solutions for a wide range of microsensors and microactuators with applications in the automotive and aerospace industries as well as in medicine, entertainment and the domestic environment; much research is being carried out in biology, drug discovery and delivery and in healthcare. MEMS devices have already led to technological breakthroughs in materials, some aspects of sustainable energy, information technology, biotechnology and national security [1–5]. It is widely accepted that MEMS

represent the next technology frontier in the new millennium after the Si-based IC industrial revolution.

Current MEMS technology is dominated by Si-based materials and the suite of fabrication technologies inherited from the microelectronics industry. Silicon has mechanical and electrical properties which make it suitable for the fabrication of MEMS devices such as gyroscopes, accelerometers and sensors. These can be integrated with electronics control circuits on the same Si substrate making them compact, efficient and energy saving. This is leading to the development of MEMS-related markets and business. However, Si has its material limitations. In particular, it has relatively low values of Young's modulus and fracture toughness; against both itself and many other materials it has

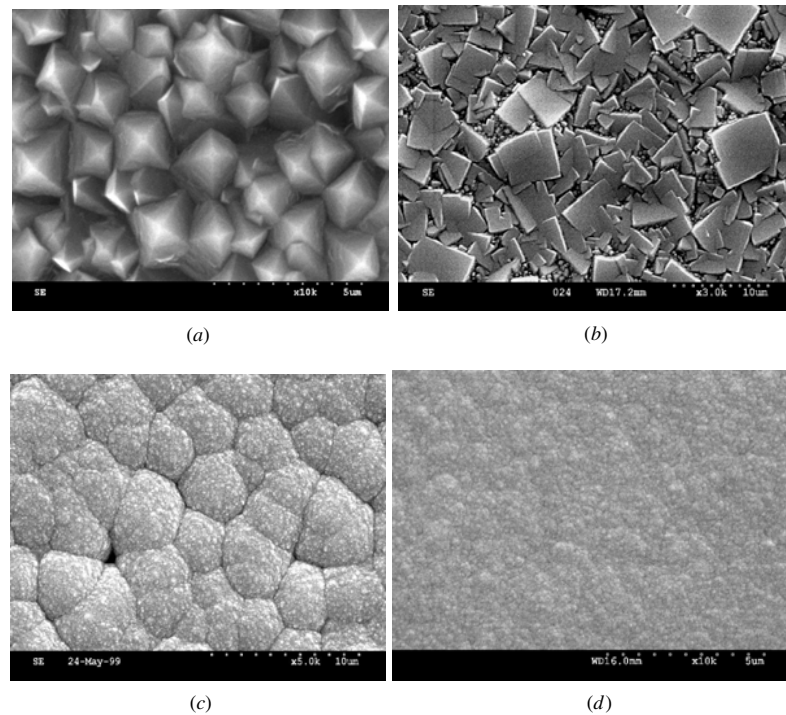


**Figure 1.** Surface morphology of diamond films with different  $\text{CH}_4/\text{H}_2$  ratios: (a) triangular  $\{111\}$  facets with a ratio of 2/98, (b) rectangular  $\{100\}$  facets with a ratio of 3/97, (c) cauliflower morphology with a ratio of 4/96, (d) a nanocrystalline diamond with a ratio of 8/92.

a comparatively large coefficient of friction (COF) and high rate of wear, and has a high surface energy and a small energy band gap. These factors can lead to a number of associated problems during both fabrication and operation. For example, microengines, rotors and linear motors that contain sliding interfaces typically suffer from rapid failure caused either by frictional wear or by stiction, i.e. unacceptably high static friction; this can be exacerbated by capillary adhesion in humid environments [6–9] or by low operation temperature and heat dissipation due to the small energy band gap.

To improve the processing techniques available to MEMS technology and to create new applications for devices, researchers continue to seek new materials for use in MEMS. Metals, semiconductors (such as SiC) and polymers (such as SU8, PMMA and PDMS) are being studied for their suitability. Among these candidate materials, diamond and diamond-like carbon (DLC) are believed to be amongst the most promising for MEMS applications. They possess a number of excellent properties that Si material and other materials lack [10, 11]. These include generally reduced coefficients of friction and increased resistance to wear, both particularly useful for microsystems containing components with sliding interfaces. Both materials have a very high Young's modulus, tensile and fracture strength, and are suitable for high frequency MEMS devices. They are chemically inert and are stable in air up to 600 °C. They have excellent thermal conductivity and low coefficients of thermal expansion (CTE) which make them useful in developing lab-on-chip devices, packages with better heat dissipation and bimorph thermal actuators with large displacements. Diamond and DLC are biocompatible, mechanically strong and tribologically effective, and as such are excellent coating materials for implantable medical

devices. DLC is hydrophobic with the ability to prevent non-specific biobinding, yet the surface can be photochemically modified to facilitate attachment of specific species, and thus DLC can be either a good base or an active material for biosensors. By suitable doping, diamond films can also be made to be electrically insulating or conducting. Diamond and DLC-based MEMS can be integrated with diamond electronics on the same substrate for high temperature applications.

Diamond and DLC in MEMS can be exploited in two ways: either as a coating material to improve and enhance the functionality of an existing MEMS design or as a structural material to deliver a unique performance that is unobtainable with other materials. This paper will review and highlight the applications of diamond and DLC in MEMS. In section 2, we will briefly introduce the methods used to grow diamond and DLC films; in section 3 we will discuss the applications of diamond and DLC films as a coating to improve MEMS performance and production yield and in section 4 we will review diamond and DLC-based MEMS devices.

## 2. Preparation and characterization of diamond and DLC films

Diamond films can be deposited using a variety of chemical vapour deposition (CVD) systems employing activation of the gases by either a microwave (MW) plasma [12–14] or a hot filament [15, 16]. Using MW-CVD, a microcrystalline (mc-) diamond film is normally grown at 600 °C to 1000 °C with a hydrocarbon gas (typically methane) in an excess of hydrogen (typical above 98%). Figure 1(a) shows a typical morphology of a microcrystalline CVD diamond film, with triangular

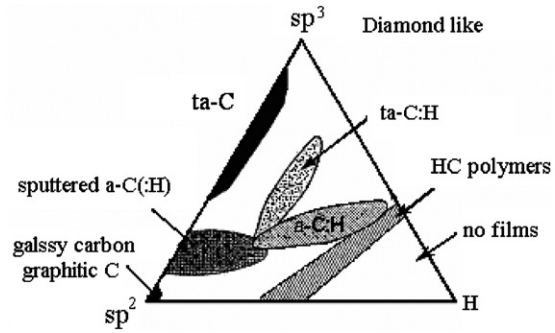
**Table 1.** Properties of DLC and diamond [10, 11].

	a-C:H	ta-C	uncd	Diamond
H (atomic%)	30	0	0	<0.1
sp <sup>3</sup> fraction	<0.5	>0.8	>0.9	~1.0
density (kg m <sup>-3</sup> )	2350	3260	3500	3515
E (GPa)	300	757	300	1145
Hardness (GPa)	<15	>20	>45	45
Residual stress (GPa)	1–2	8–10	0	0

{111} facets. With an increase in the relative concentration of CH<sub>4</sub> in the precursor gas mixture, and/or the substrate temperature, square and rectangular forms of {100} facets begin to dominate as shown in figure 1(b). Under a higher (>2%) methane concentration, a ‘cauliflower’ morphology can be obtained (see figure 1(c)). A further increase in CH<sub>4</sub> partial pressures results in nanocrystalline (nc-) diamond as shown in figure 1(d) as grown by one of the authors.

Potential problems associated with the micro- and nanocrystalline diamond films for MEMS applications include high deposition temperatures, low deposition rates, large intrinsic and thermal stresses, poor adhesion to the substrate and a high value of surface roughness [12–14]. The development of ultra-nanocrystalline (unc-) diamond technology by Argonne National Laboratory has solved some of these problems [6, 17–19]. Unc-diamond films are synthesized using MW-PECVD with argon-rich Ar (99%)/CH<sub>4</sub> plasma chemistries at a temperature of 400 °C; the resulting films consist of diamond grains 3–5 nm in diameter with atomically abrupt grain boundaries that consist of carbon atoms in a mixture of sp<sup>3</sup> (diamond), sp<sup>2</sup> (graphite) and intermediates. This unique nanostructure results in very smooth as-deposited surfaces with excellent mechanical properties, low stress and good adhesion to the substrate [18–20]—all promising for MEMS applications. Unc-diamond films can be used directly as structural materials for MEMS devices, whereas mc-diamond films may require polishing to obtain a smooth surface before being used. Table 1 shows some material properties for such diamond films.

The possibility of doping diamond, and thus changing it from being an insulator into a semiconductor, opens up a whole range of potential electronic and MEMS applications. Diamond films are promising for high-performance MEMS-based telecommunication devices, high-definition flat panel displays, radiation detectors, surface acoustic wave (SAW) devices and biosensors, as discussed in the following sections. However, there are a number of major problems that need to be overcome for the successful application of this material. CVD diamond films are polycrystalline and hence contain grain boundaries, twins, stacking faults, and other defects, which all reduce the lifetime and mobilities of carriers. Traditionally, electrical conductivity of diamond films is obtained through doping with boron achieved by adding a few per cent of B<sub>2</sub>H<sub>6</sub> to the CVD process gas mixture during growth, which results in p-type behaviour [21, 22]. At low and medium concentration, the activation energy for doping is low and is suitable for electronics applications, particularly in high temperature. However, n-type doping is still a problem for diamond films. Phosphorous has been used as an n-type dopant with an activation energy of ~0.6 eV, but high doping concentrations

**Figure 2.** Ternary phase diagram defining the different regions of diamond-like carbon materials.

can cause severe internal stresses due to the large difference in the atom sizes of P and C [23, 24]: this difficulty has severely limited its widespread application. Recently, nitrogen has been proposed as an alternative to phosphorous in doping of ultra-nanocrystalline diamond [25, 26]. Nitrogen doping leads to n-type conduction with a low activation energy. Although the mechanism of nitrogen doping is yet to be clarified, it opens widespread applications of diamond in both electronics and MEMS. An n-type unc-diamond has been combined with a p-type diamond to form pn-heterojunction which is the basic building element for electronics [27]. Conductive unc-diamond has been successfully used as the heater for water microjets [28]. Hereafter, we use the term diamond to refer to such mc-, nc- and unc-diamond materials so as to distinguish them from diamond-like carbon films.

Diamond-like carbon is a family of carbon-based materials containing a mixture of sp<sup>2</sup> (graphitic) and sp<sup>3</sup> (diamond) carbon phases. Depending on the deposition methods used, some hydrogen atoms can be included in the DLC film. The amount of hydrogen contained, as an atomic percentage, varies from zero to more than 50%. Generally speaking, mechanical properties and wear resistance deteriorate as the hydrogen content increases (and the proportion of sp<sup>3</sup> bond decreases) but the surface energy and coefficient of friction decrease due to greater hydrogen passivation of the surface carbon dangling bonds. The ternary phase diagram shown in figure 2 defines regions of pure carbon (designated a-C), tetrahedral amorphous carbon (ta-C) and hydrogenated carbon (a-C:H) with the corresponding extent of hydrogenation. Some properties of such DLC films are summarized in table 1.

Several methods have been developed for producing DLC films. Plasma-enhanced (PE) CVD techniques employing radio frequency (RF) and dc glow discharges in hydrocarbon gas mixtures produce smooth amorphous carbon and hydrocarbon films, which have a mixture of sp<sup>2</sup> and sp<sup>3</sup> bonds. PECVD produces hydrogenated amorphous carbon (a-C:H) with reasonable deposition rates and good uniformity, and is suited for very large-scale production. Ion beam deposition of DLC films has the advantage of being able to deposit high quality coatings at very low temperatures (near room temperature). The disadvantages are that the deposition rate is very low and that the substrates need complex manipulation to ensure uniform deposition. Sputtering from a graphite target, with or without the presence of hydrogen

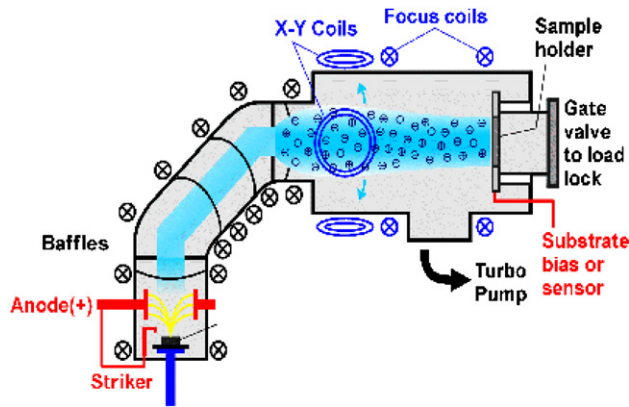


Figure 3. Schematic illustration of the FCVA system (after [30]).

gas, offers another route to deposit DLC or a-C:H films. Depending on facilities, or the power and bias used, sputtering can grow DLC films with  $sp^3$  ratios of up to  $\sim 50\%$ . Generally speaking, sputtered DLC films have a high quantity of  $sp^2$  bonds and a low mechanical strength because of the low ion energies involved during deposition which makes sputtered DLC films attractive as solid lubricants. Laser ablation of graphite under vacuum leads to the condensation of high-energy carbon atoms, ions and clusters onto the substrate. The high energy of the incident particles provides the driving force to convert  $sp^2$  (graphite) into  $sp^3$  (diamond) bonded carbon. The deposited films are extremely smooth (on the tenth of nm scale), hydrogen free and are termed amorphous carbon (a-C). Ablation of polymeric targets such as polycarbonate or polymethyl methacrylate (PMMA or perspex) under vacuum or in the presence of hydrogen provides another method to grow DLC films [29]. The advantage of laser ablation is that it is a low temperature process which makes this technology compatible with both delicate microelectronic circuitry and silica glass substrates. However, there are problems associated with film uniformity over the deposited area.

Filtered cathodic vacuum arcs (FCVA) can be used to deposit DLC films from a pure graphite target in a high vacuum with a typical configuration shown in figure 3 [30]. Carbon ions are generated by striking the graphite target at high voltage and are subsequently extracted and accelerated through a magnetic field before being deposited on a substrate. This apparatus produces pure amorphous carbon films with a high  $sp^3$  fraction owing to the high-energy ions involved. These films are typically tetrahedral in structure and are designated as ta-C. They significantly differ from the hydrogenated carbon films in terms of their material properties (see table 1). They possess both a high Young's modulus of up to 800 GPa and a high hardness of  $\sim 60$  GPa. Implementation of a magnetic field and a  $90^\circ$  curved particle filter removes carbon clusters (or large particles) and allows the deposition of ultra-smooth ta-C films with rms surface roughness approaching 0.1 nm regardless of the thickness of the films [31].

The material properties of the DLC films grown by FCVA, such as Young's modulus, hardness and tensile strength, are strongly affected by the  $sp^3$  bond content which can be varied significantly by changing the energy of the  $C^+$  ions. The proportion of  $sp^3$  bonds initially increases sharply with increasing C-ion energy, but then gradually decreases.

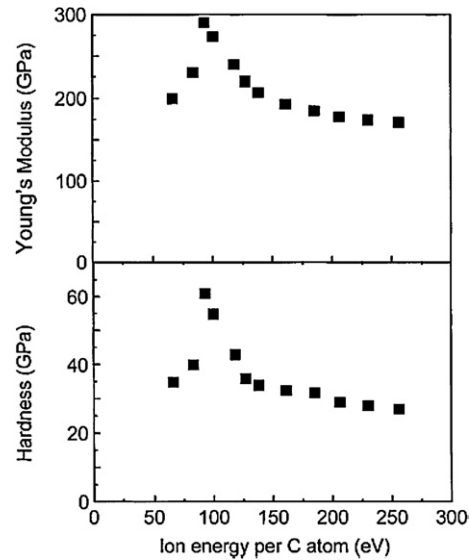
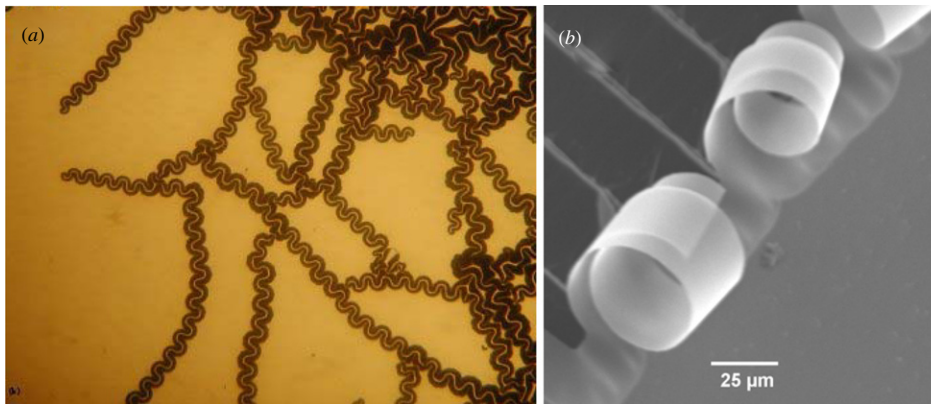


Figure 4. Film hardness as a function of ion-energy for a FCVA DLC film ([32], with permission to reprint obtained from The America Physics Society).

Hardness, residual stress and Young's modulus follow the same trends with the change in energy of the  $C^+$  ions [32]. Since there are high-energy ions involved in the film deposition, DLC films (especially those grown by FCVA) possess very large compressive stresses of up to 10 GPa [33]. The highest hardness and the highest residual stress in the film are achieved at the highest  $sp^3$  content which is typically obtained at an ion energy of the order of  $\sim 100$  eV, as shown in figure 4. Ions with higher energy penetrate deeper into the film causing thermal spiking. This leads to relaxation and the formation of  $sp^2$  bonds, rather than  $sp^3$  bonds; consequently hardness decreases. Because of the large compressive stress, delamination of DLC films from the substrate can be a major problem when the film thickness exceeds some critical value. Figure 5(a) show a micrograph of a typical delaminated DLC film on a Si substrate. Stress gradients exist in DLC films owing to the subimplantation of  $C^+$  ions of high energy, and these can cause severe bending of DLC structures once they are released from the substrate. Figure 5(b) shows several DLC cantilevers (80 nm thick) made by a laser cutting and released by removing the silicon underneath using  $SF_6$  plasma etch by the authors [34]. All the cantilevers curl significantly with a radius of curvature of less than  $40 \mu\text{m}$ .

As a structural material for MEMS, stress-free DLC films with a defined thickness are required. Several approaches have been developed to obtain thick DLC films with low values of internal stress. Doping DLC with B, Si, N species or transient metals up to a few per cent by volume can reduce the stress dramatically [35, 36]. However, this technique generally also leads to a reduction in Young's modulus and hardness. Post-deposition annealing of the DLC films in a vacuum or in  $N_2$  can reduce film stress; for example, it has been reported that annealing at  $600^\circ\text{C}$  for 10 min can eliminate  $\sim 90\%$  of the stress in DLC films [35, 37]. However, annealing at high temperature is not feasible in the fabrication of many MEMS devices: the decrease in film stress through post-annealing is





**Figure 5.** Large film stress and gradient stress in DLC films: (a) stress induces delamination of a DLC layer on a Si substrate, (b) curled DLC cantilevers made by laser cutting and KOH wet etch.

also limited, leading to a final residual stress typically in the range of a few tens of MPa to a few hundred of MPa.

Improvement in low stress DLC films can be achieved in a nanostructured DLC layer by depositing a sequence of alternating harder ta-C and softer a-C:H layers [38]. In this way it may be possible to build up a sufficient thickness for a DLC film to be used as a structural material. Also, improved FCVA systems are now available to grow stress-free ta-C films. These either use a pulsed bias applied to the substrate during deposition or a pulsed ion source for growth. Stress is relaxed when the pulse is off, so a stress free film up to a few micrometres can be achieved [39]. In high mechanical stress applications, adhesion of the DLC film to the substrate is of paramount importance. This problem has now been largely overcome by ensuring that there are no stress concentrations near the coating/substrate interface. For example, a graded interlayer design (Ti/TiN/TiCN/TiC/DLC) has been proposed prior to deposition of DLC [40]. This ensures that there are no abrupt changes in composition and that the stress is introduced into the film gradually. Recently, a nanocomposite film design was proposed with the aim of obtaining a film with both low stress and high toughness, while maintaining a reasonably high hardness and modulus [41]. As shown in figure 6, by co-deposition of Si or metal targets with a graphite target, nanocrystals of silicon carbide or metal carbide, such as TiC or CrC, are embedded into an amorphous carbon matrix that is typically doped with aluminium. The large compressive stress in the film is significantly relieved by the Al doping, while nanocrystals of carbide can enhance the hardness and modulus [40]. Hereafter, the term of DLC refers these amorphous carbons.

### 3. DLC as a surface coating for MEMS

#### 3.1. Anti-stiction coating

As the dimensions of devices scale down, the surface-to-volume ratio increases rapidly and surface phenomena become much more significant. Forces associated with surface phenomena such as Van der Waal's attraction, capillarity and local shear due to viscosity become predominant at the microscale. MEMS devices typically have overall dimensions

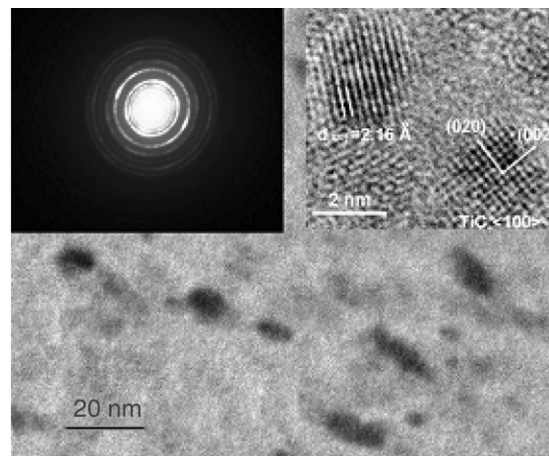


**Figure 6.** TEM morphology of a nanocomposite TiC/Al/DLC film with nanocrystalline TiC particles embedded inside Al-doped DLC matrix.

ranging from tens of micrometres to a few millimetres, and the separation of individual elements (determined by the thickness of the sacrificial layer) is in the range of submicrometre to less than a few micrometres. In these cases, surface adhesion and friction potentially dominate the performance of MEMS devices [8, 42–44]. Adhesion causes low production yield and reproducibility problems in fabrication, while friction and wear may lead to premature failure and limited lifetime.

Conventional microelectronic fabrication provides reliable processes for MEMS fabrication only up to the stage at which the sacrificial layer is removed. This unique process is required to release any moving components from the substrate and so provide the articulation necessary. SiO<sub>2</sub> is the predominant sacrificial material in Si-based MEMS and can be removed by a simple wet etching process. However, at such small surface separations, capillary-induced adhesion forces may be sufficiently strong to pull down freestanding components so that they come into contact with and stick to the substrate so jeopardizing the intended functionalities of the device. This can have a tremendous effect on fabrication yield and device reproducibility. New processes have been developed to counteract this effect such as freeze releasing, HF vapour etching and dry reactive ion etching. However, even

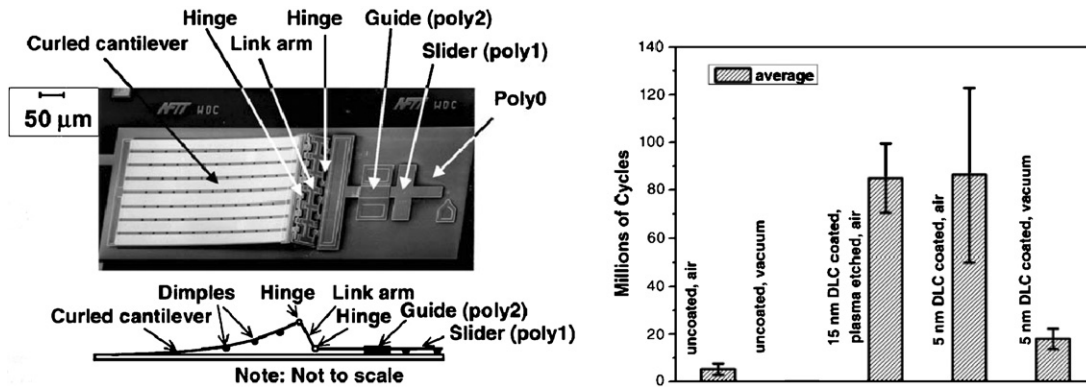


**Figure 7.** SEM micrograph of an electrostatic lateral motor used to test the wear rate of the DLC coating (left); the lower left is a side view of the linear motor. A comparison of sliding cycles of the motor with and without DLC coating (right) ([46], permission to reprint obtained from Elsevier).

**Table 2.** Frictional and wear properties of DLC [48, 51].

Carbon film grown in	COF	$K_w$ mm <sup>3</sup> N <sup>-1</sup> m <sup>-1</sup>
100% CH <sub>4</sub>	0.015	$9.0 \times 10^{-9}$
25% H <sub>2</sub> + 75% CH <sub>4</sub>	0.01	$7.36 \times 10^{-9}$
50% H <sub>2</sub> + 50% CH <sub>4</sub>	0.004	$1.23 \times 10^{-8}$
90% H <sub>2</sub> + 10% CH <sub>4</sub>	0.004	$2.8 \times 10^{-10}$
100% C <sub>2</sub> H <sub>2</sub>	0.27	$7.5 \times 10^{-7}$
Hydrogen free DLC	0.25	$2.8 \times 10^{-7}$
Diamond	0.07	n/a

after a successful fabrication, the same adhesion mechanism can cause freestanding structures to collapse during operation in a humid environment, as moisture can condense easily in the narrow separation of typical MEMS. Diamond and DLC have low surface energies and large contact angles  $\sim 90^\circ$ : this reduces the propensity of freestanding components to adhere to the substrate, thus significantly improving production yield, reliability and lifetime.

### 3.2. Tribological coating

Microactuators with moving parts, such as microengines, gears and bearings, will experience surface contact during operation. At the microscale, viscous shear forces are exceptionally high, so provision of a liquid lubricant is no longer a feasible way to reduce friction. The pairing of Si and Si has a high coefficient of friction up to 0.6 and, in addition, MEMS devices made from Si can suffer from a high wear rate during operation [8, 9]. For example, the literature contains reports of Si-based microengines and micromotors that could only be operated for a few minutes—if not seconds—before failing because of tribological collapse [6–9]. DLC films have very low COFs and their wear rate  $K$  (measured as a wear volume per unit load per unit sliding distance) is exceptionally small which make them potentially excellent solid lubricants for MEMS devices. Table 2 provides a summary of the measured COF and  $K$  values for a number of DLC films with different hydrogen contents. Hydrogenated DLC has a low COF and  $K$  as hydrogen passivates the dangling bonds on the surface making it super-lubricious. The smooth surface of the film is the other key factor for the low COF and  $K$ . To reduce the friction and wear in many MEMS devices, conformal deposition of

diamond and DLC films by CVD or PECVD is desirable. For MEMS devices with partial sliding surfaces, it is still possible to have non-conformal diamond and DLC films as the coating to minimize the friction and wear.

Great efforts have been made to reduce the friction and wear of MEMS devices by using DLC and UNCD films [45–47]. PECVD DLC coatings have been used to improve the lifetime of linear motors that are actuated by electrostatic forces which drive a sliding component laterally [46]. Figure 7(a) shows an SEM picture of the linear motor used for these experiments. Sliders coated with DLC layers of 5–15 nm thick had prolonged lifetimes of 15–80 million cycles, more than 300 times that of those without the DLC protective coating, as shown in figure 7(b). These results clearly demonstrated the superiority of DLC as a low friction and high wear resistant coating.

Other surfaces such as fluorine-based materials epitomized by Teflon or those coated by self-assembled monolayers (SAMs) can display low friction coefficients, and both may be used in MEMS devices to improve reliability. However, DLC films have the particular attraction of a combination of high mechanical strength, chemical inertness and good biocompatibility.

Although most MEMS actuators are not used in corrosive chemical atmospheres, they can still interact with the environment through physical adsorption. This mechanism can introduce significant fluctuations in frictional and wear resistance. In the case of a hydrogenated carbon a-C:H film sliding against a similar surface, the COF depends strongly on the relative humidity, as shown in figure 8. Values of COF below 0.05 are obtained in dry air (or vacuum) with hydrogenated carbon films, but these increase by a factor of 3 or more as the relative humidity increases. The COF also appears to be influenced by the ratio of H:C in the precursor gas used during deposition. Tetrahedral ta-C films behave differently from those of a-C:H. They have higher COFs in vacuum or dry air, but this appears to remain broadly constant, or at least not increase significantly, in the presence of increasing humidity [11, 48, 49].

When discussing the tribological properties of DLC, it is important to take account of the nature of the counterface. For a number of different counterface materials (including steel, silicon nitride and sapphire), long-term stability appears

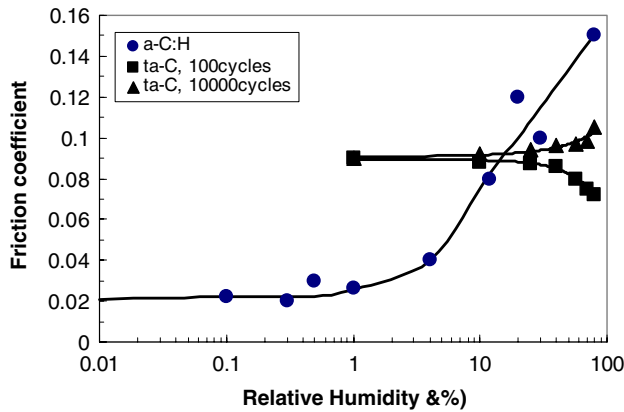


**Figure 8.** Variation of frictional coefficient with relative humidity for a-C:H and ta-C ([11, 49], after J Robertson and A A Voevodin).

dependent on the formation of a carbon-rich transfer layer derived from the DLC [11, 50]. This transfer layer possesses a distinctive morphology of its own, often consisting of fine graphitic nano-particles (<5 nm) within a distorted diamond-like structure. If both the extrinsic or environmental factors and the intrinsic properties of the films and underlying substrates can be optimized, it is possible to generate extraordinarily low values of both COF and specific wear rates, as indicated in table 2.

Recently, the authors performed a series of tests on a FCVA ta-C coating using a piezo-actuated microtribometer and 1 mm sapphire ball as the counterface [52]. The thickness of the DLC coating on the Si substrate was 50 nm and the contact pressure was in the range of 1–2 GPa. The COF under various loads is shown in figure 9(a). The results indicated that the initial COF increases with applied load although, in all cases, after about 500 cycles the COF dropped significantly to a final value of about 0.02 to 0.04. This decrease in COF is attributed to the development of a thin carbon-rich transfer layer on the surface of the sapphire ball as shown in figure 9(b). This soft carbon layer acts as a buffer between the two harder underlying surfaces to prevent hard asperity-to-asperity contact and increases the effective contact area, causing the frictional force to reduce. Similar results were reported in [53] with silicon nitride balls.

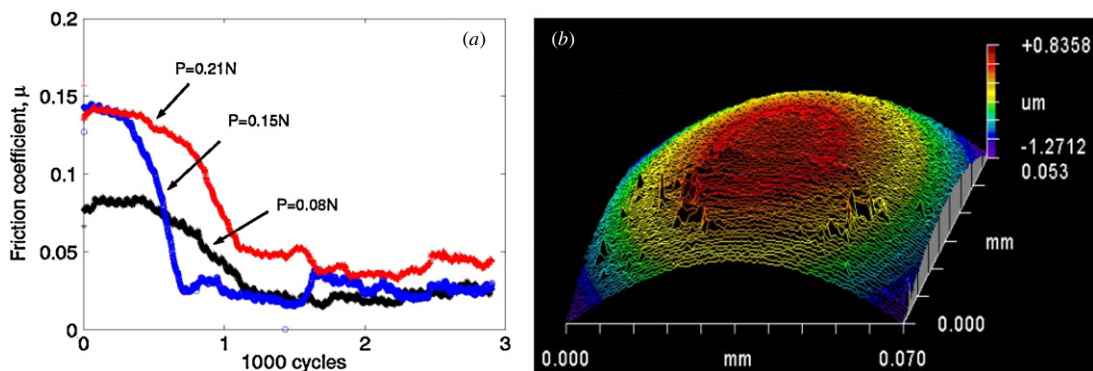


**Figure 9.** (a) Frictional behaviour of ta-C (50 nm) under ambient conditions against a sapphire ball. (b) Material transfer to sapphire ball after tests on ta-C films under a load of 0.2 N for 3000 cycles. The spiking features are the transferred carbon material on the ball surface.

### 3.3. Bio-chemical coatings and bio-interface for sensors

As a result of their good chemical resistance, temperature stability and biocompatibility, diamond and DLC films have found widespread application in biological coatings for implantable medical devices, particularly in two specific areas: (1) when the surfaces in question make contact with blood such as heart valves and stents and (2) when the surfaces are subject to mechanical loading which can lead to unacceptable levels of wear as in joint prostheses. Any implanted device must not trigger the body's immune defence systems; otherwise it is likely to be encapsulated by liposites or macrophages and rendered inoperative. A further key issue is the ability of the implant surface to inhibit thrombus formation. The biological behaviour of an implant is strongly influenced by the chemical environment at its surface. Bioreaction can be tuned by modifying the surface chemistry especially the element composition. DLC can be easily alloyed with other biocompatible materials such as titanium as well as toxic materials such as silver, copper and vanadium by normal co-deposition methods [54]. *In vitro* experiments have shown that DLC surfaces have a much better ability to suppress thrombus formation than glassy carbon, a material widely used for heart valves. Nanocrystalline diamond-coated medical steel has shown a high level resistance to blood platelet adhesion and thrombi formation [55].

Diamond and DLC coatings have successfully been used to improve the wear resistance of implanted medical devices as they offer excellent mechanical, tribological and anti-corrosion protection. Their use has been proposed for applications as diverse as artificial heart valves, prosthetic pins, roots of false teeth, surgical scalpels and dental instruments [56–59]. As these bio-medical applications of DLC are beyond the scope of this paper, they will not be discussed in detail; for an introduction to these applications, see review articles by Grill [56], Hubert [57], Freitas [58] and Dearnley [59].

Recent bio-medical applications have involved the direct application of DLC as a bioactive surface for bio-interfacing and biosensing [60–62], as exemplified by polymerase chain reaction (PCR) devices. Many applications in the life sciences involve biologically modified surfaces that must



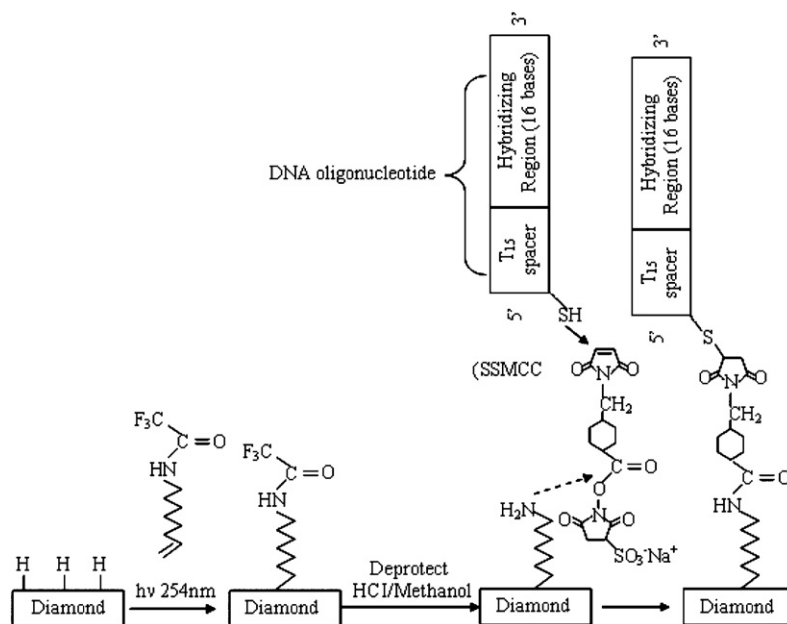


**Figure 10.** Schematic drawing of the photochemical surface modification and subsequent covalent attachment of DNA on a diamond surface ([65], after R J Hamers).

be stable in contact with electrolytes for long periods of continuous use. Lack of stability of many potential biological devices has limited their successful application. Excellent stability in harsh chemical and biological environments makes diamond and DLC strong candidates as interfaces to biological molecules and systems. Diamond and DLC surfaces when terminated with hydrogen are highly hydrophobic, and this hydrophobicity can be controlled through post-deposition processing. Diamond and DLC surfaces resist non-specific DNA and protein surface binding, a critical requirement for high sensitive biosensor detection. DNA immobilization experiments on various materials have confirmed that nanocrystalline diamond surfaces have a much better resistance to non-specific binding than other materials such as polymers and bare silicon [60].

Hydrogen-terminated diamond and DLC surfaces can be photochemically modified for the attachment of amine linker molecules which can then be adjusted to deliver bio-molecular recognition properties and so control the non-specific binding of DNA and proteins to the surface [61, 63–66], a key process in enabling bio-detection. This behaviour can be utilized to develop various label-free biosensors such as acoustic wave-based sensors, field effect devices and cantilever resonator sensors as will be discussed in detail later. Figure 10 shows the sequence in the photochemical modification of the surface of diamond and DLC films used for biobinding. Polycarbonate and dialysis membranes coated with nanocrystalline diamond have shown enhanced enzyme electrode performance in terms of haemocompatibility and permeability with a dramatic reduction in the adhesion of red blood cells [63].

The attachment of enzymes, DNA or proteins to either diamond or DLC films leads to a drastic change in their physical properties, and thus they can be used as biologically specific electrodes in the development of particular electrochemical biosensors. These can realise

biosensing through measurements of impedance spectroscopy, resonant frequency shift or other electrical signals [17].

The attachment of DNA molecules typically leads to changes in the electrical properties of the interface as the negative charge on the DNA alters conductivity in the diamond. This has been utilized to realise molecular field effect biosensors [59]. Glucose sensors were recently developed which directly utilized conductive unc-diamond thin film as the electrodes through which glucose oxidase enzymes were covalently immobilized. This demonstrated that conductive diamond could serve as a robust platform for a new class of bio-interface which may prove particularly useful in implantable biosensors and devices [67, 68]. Diamond is sensitive to UV light of wavelength  $<224$  nm as it has an indirect band gap of 5.45 eV, whereas many bio-molecules display a high absorption of UV light. This has led to the development of novel diamond biosensors. DNA fragments are arranged in agarose gels, and the UV light passes through the gel [69]. Absorption of certain UV wavelengths by specific DNA fragments can be detected by arrays of diamond UV detectors; thus specific DNA fragments can be identified and quantified with a detection limitation down to  $\sim 1$  ng. The main disadvantage of this technique is that it is limited to certain DNA fragments which absorb particular UV wavelengths. It is believed that in the near future, we will see the realization of prototype diamond and DLC-based biosensors for applications ranging from biosensors and MEMS-based arrays to gene-chips and proteomics [67].

#### 4. DLC as structural materials

The most attractive properties of diamond and DLC when used as structural materials for MEMS are their high Young's modulus, hardness, high thermal conductivity and low coefficient of thermal expansion (CTE). Diamond and DLC have been successfully utilized as a structural material for



cantilevers and comb-drives with high resonant frequencies, as bimorph structures which take advantage of their low CTE, for micro-encapsulation and MEMS packaging which maximizes the heat dissipation for microelectronic applications, and as microgears and linear motors which exploit both their low COF and high wear resistance. In this section, a number of DLC-based MEMS devices—both sensors and actuators—will be presented.

#### 4.1. High frequency resonators

Simple cantilevers, double-clamped beams and comb-drivers are basic MEMS components, and are regularly used to construct various microsystems and sensors. Cantilever sensors can use both their mechanical deflection and the shift in their resonant frequency to perform sensing. The sensitivity of a cantilever-based sensor is proportional to its resonant frequency so that devices with a high resonant frequency have a high resolution: this means that only a minimal amount of target molecule when attached to the surface of the cantilever can cause a large shift in its resonant frequency. Assuming a cantilever with a cross-section of  $A$  and length  $L$ , the resonant frequency  $\omega$  is given by

$$\omega = \sqrt{\frac{EI/L^3}{\rho LA}} = \sqrt{\frac{E}{\rho}} \times \frac{\sqrt{A}}{L^2}, \quad (1)$$

where  $E$  and  $\rho$  are material's Young's modulus and density, respectively. Equation (1) shows that there are two ways to increase the resonant frequency of a device: either by selecting appropriate materials,  $E/\rho$  is a figure of merit for potential materials, or by changing the physical dimensions. Making the cantilever shorter is one way to increase the frequency of the device, but a cantilever with an adequate size is necessary for optical alignment (typically, a laser beam is used to detect the resonant frequency) and for the attachment of a sufficient amount of the biologically active molecules used for detection.

The Ashby engineering material selection method has been widely used in macro-component engineering [70] and can be extended to select materials for MEMS devices [71, 72]. Figure 11(a) shows a map with axes of Young's modulus and density for different materials. The dotted lines represent fixed ratios of the parameter  $\sqrt{E/\rho}$  so materials located towards the top left of the chart have high values of  $E/\rho$ . Cantilevers made from these materials will therefore have higher resonant frequencies. At the top of the chart is the diamond, which illustrates that this and related materials are the best choice for resonators with the highest frequencies. The same principle of material selection can be applied to comb-driver and double-clamped MEMS devices.

Fabrication of diamond and DLC-based cantilevers and comb-drivers have been reported in the literature [39, 73–76]. Figure 12 shows a SEM picture of an array of DLC cantilevers and their associated frequency response. The DLC layer was grown by a pulsed FCVA system to a thickness of 1.8  $\mu\text{m}$ . The resonant frequency of each cantilever was measured at 108 MHz, roughly double that of Si cantilevers of the same dimensions [39]. Moreover, the quality factor of the DLC cantilevers is very high, showing the potential for high frequency device applications. Double-clamped nano-beams made from unc-diamond with a width of 60 nm have similarly

demonstrated sharp resonant peaks, with resonant frequency up to 640 MHz [76].

The same principle has also been applied to other microsensors to improve their performance [77]. A piezoelectric bimorph cantilever consisting of diamond and  $\text{Al}_2\text{O}_3$  layers showed a much enhanced sensitivity under high pressures. Piezoelectric actuators have the advantages of being capable of self-sensing and self-actuating. The use of diamond layers with their high elastic modulus can improve both resonant frequency and device sensitivity.

For sensor applications, resonators such as cantilevers and comb-drivers are normally excited at their resonant state. Resonators with high quality factors will have high resolution and small detection limitations. Suppression of energy loss is the key to obtaining high quality factors. The operation of resonators at low pressure is a general way to reduce external energy loss due to the reduction of viscous damping. Improvement in the  $Q$  factor can also be achieved by selecting a material with a low intrinsic energy loss. Such losses, arising from thermal elastic dissipation of energy, are correlated with the magnitude of the coefficient of thermal expansion. Consequently, since diamond and related materials have low CTEs, the quality factor of diamond and DLC-based cantilevers is expected to be at least one order of magnitude higher than that of Si and metals-based resonators [78]. Figure 13 shows the theoretical comparison of the quality factors of Si and diamond, i.e. poly-C, cantilevers.

Surface acoustic wave devices are another family of sensors employing the detection of resonant frequency as the sensing mechanism and have already been used to detect various bio-species such as DNA and proteins. The sensitivity  $e$  of a SAW device is proportional to the resonant frequency  $f$  raised to some power, i.e.  $e \propto f^\gamma$  (where  $1 < \gamma < 2$ ). For better detection with small detection limitations, SAW devices also require high quality factors. Thin-film piezoelectric materials, such as ZnO and AlN, on Si substrates have been used to construct SAW sensors at a low cost; however, Si is a 'soft' material, which reduces the acoustic speed in the piezoelectric materials. This causes the resonant frequency to be low and therefore the quality factor to be poor. Diamond and DLC films can be used to 'harden' the Si substrate or to trap the acoustic wave inside the poly-C layers which have  $\sim 4$  times higher acoustic speed; hence both the resonant frequency and detection sensitivity increase. When hardening with a DLC layer, both simulation and experiments have shown improvements in acoustic speed by a factor of 2–3 compared to those in ZnO and AlN [79, 80].

Since mc-diamond films are comparatively rough, special techniques are required to obtain surfaces sufficiently flat for the fabrication of SAW devices. A double-layer diamond deposition process, with the Si substrate removed, to form freestanding structures of ZnO/diamond for SAW devices has demonstrated an acoustic wave speed of 9696  $\text{m s}^{-1}$  and effective coupling  $K^2 = 0.75\%$  [79]. On the other hand, DLC films are typically sufficiently smooth for the direct fabrication of SAW devices, and have received great attention in this application. Figure 14 shows a typical cross-section of a ZnO/DLC SAW structure on a Si substrate [81]. Such devices can have a DLC layer either on top of the piezoelectric material [82] or beneath it [81], and

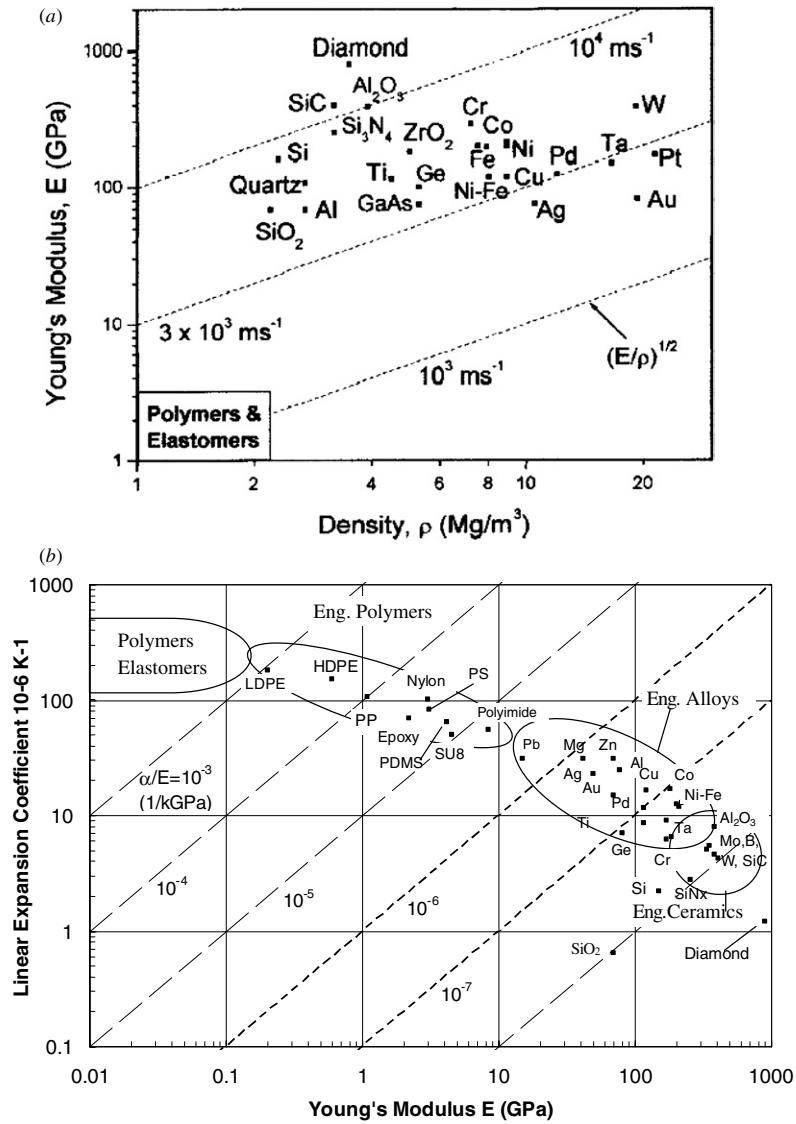


**Figure 11.** Relationship between (a) Young’s modulus and density, and (b) linear expansion coefficient and Young’s modulus for materials used for engineering purpose ([71], courtesy of Dr Srikar, permission to reprint obtained from IEEE).

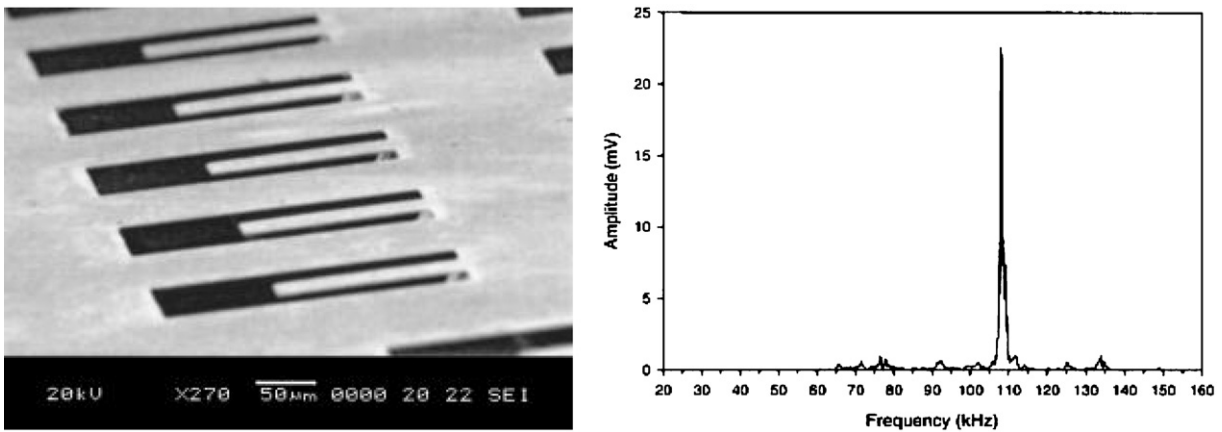


**Figure 12.** DLC cantilever and its frequency response ([39], permission to reprint obtained from AVS The Science and Technology Society).

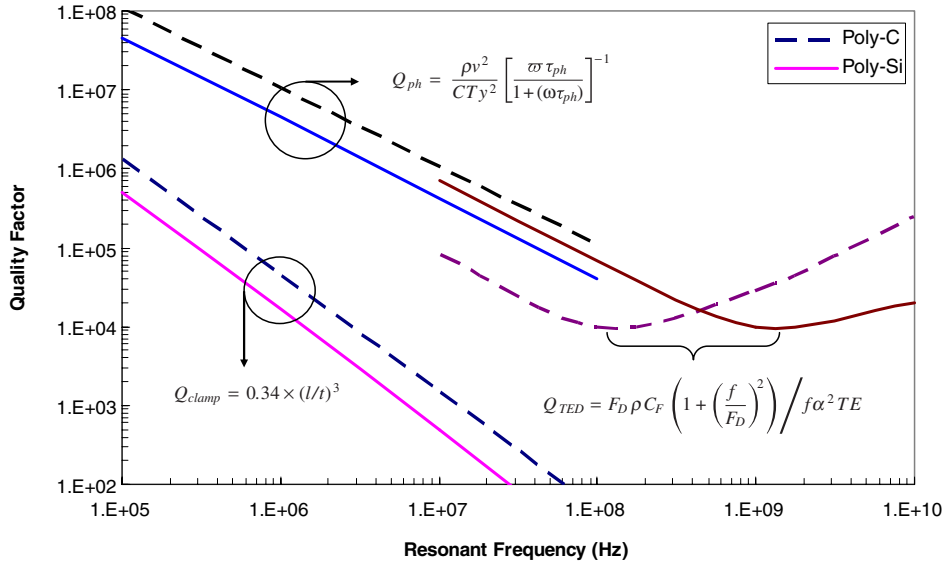


Figure 13. A comparison of quality factor for Si and diamond (poly-C) cantilever resonators with a function of frequency (after [78]).

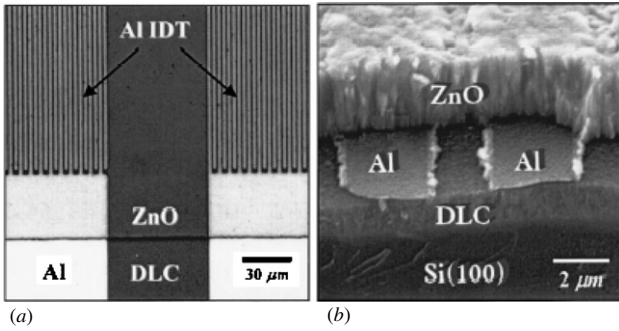


Figure 14. ZnO/DLC SAW structure ([81], permission to reprint the figure obtained from AVS The Science & Technology Society).

have achieved acoustic wave velocities in the range of 5000–11430 m s<sup>-1</sup>; these are substantially higher than those in ZnO films and clearly demonstrate the feasibility of fabricating gigahertz SAW devices on low acoustic wave substrates for RF-communication applications with the potential to be integrated with conventional CMOS manufacture.

#### 4.2. Thermal actuators and other MEMS devices

Microthermal actuators have the dual advantages of generating both large forces and displacements and so find application in microsystems. There are two basic forms of microthermal actuators. One is based on a bilayer structure which delivers an out-of-plane motion [83], whereas the other is the shape bimorph structure made from a single material [84] and is often called ‘heatuator’. This produces an in-plane motion through the differential thermal expansion of a pair of linked beams—one thin and the other considerably wider. The bilayer consists of two layers of materials with different coefficients of thermal expansion  $\alpha_s$  and  $\alpha_f$ . At temperature  $\Delta T$  the bilayer beam curls, say to a radius  $R$ , such that [85]

$$\frac{1}{R} = \frac{6(\alpha_s - \alpha_f)\Delta T E_f t_f}{E_s t_s^2}, \quad (2)$$

where  $(\alpha_s - \alpha_f)\Delta T$  is the thermal strain. In equation (2)  $t_s$  and  $t_f$ ,  $E_s$  and  $E_f$  are the thicknesses and Young’s modulus of the bottom and top layers, respectively. The tip displacement  $\Delta y$  of the bilayer beam is expressed as

$$\begin{aligned} \Delta y &= \frac{L^2}{2R} = \frac{3(\alpha_s - \alpha_f)\Delta T E_f t_f L^2}{E_s t_s^2} \\ &= \frac{(\alpha_s - \alpha_f)E_f}{E_s} \times \frac{3\Delta T t_f L^2}{t_s^2}. \end{aligned} \quad (3)$$

The deflection of a heatuator is given by [86, 87]

$$d \propto \frac{\alpha \Delta T_{ave}}{E} = \frac{\alpha V^2}{12k\rho E} = \frac{\alpha}{kE} \times \frac{PL}{12A}. \quad (4)$$

It is clear from the equations that the deflection of a bilayer actuator is proportional to the difference in CTE of the materials used. DLC has a very small CTE  $\sim 10^{-6}$  K<sup>-1</sup> and so is one of the most attractive materials for bilayer thermal actuators when used in combination with materials with high CTEs. On the other hand, the deflection of a heatuator is proportional to the CTE of the single material used, and the larger the CTE, the greater the displacement it can deliver. Diamond and related materials are not suitable for the fabrication of heatuator thermal actuators as they not only have a small CTE but also have a large thermal conductivity  $k$  and large elastic modulus  $E$ ; both reduce  $d$  as indicated by equation (4). Figure 11(b) shows the relationship between the linear expansion coefficient and Young’s modulus for various materials. Lines of constant slope represent fixed ratios of the parameter  $\alpha/E$ . Materials widely separated in the chart will be suitable for bilayer thermal actuators. Those towards the upleft of the chart have a high value of  $\alpha/E$  and thus are suitable for the fabrication of high-performance heatuators.

High values of both tensile strength and elastic modulus make diamond and related poly-C materials excellent candidates for high speed and contact-mode microactuators. They have consequently been used to fabricate various MEMS devices, such as the gears, microengines, rotors and accelerometers as shown in figures 15 [6] and 16 by one of authors [88].



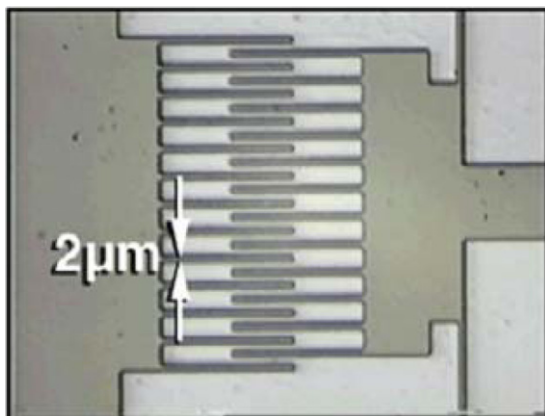


**Figure 15.** Optical photo of a comb-driver made from the unc-diamond film ([6], permission to reprint obtained from Sardia National Laboratory).

Radio-frequency capacitive MEMS switches have great potential in RF communications because of their high isolation and low power consumption. Such a device typically has a bridge (or a cantilever) electrode overhanging a bottom electrode which is covered with a dielectric material. When a voltage is applied to the bottom electrode, the bridge electrode is pulled down and makes contact directly with it. The signal is capacitively coupled to the ground, i.e. the off-state. However, charges are injected and stored in the dielectric due to the sudden increase in the electrical field and can lead to premature failure of the device. Leaky diamond films have been successfully used in RF capacitive MEMS switches with negligible RF loss up to 65 GHz owing to the excellent electrical properties of the diamond layer [89]; the leaky behaviour of the diamond layer provides the film a conductive path for any potential trapped charges thus eliminating the problems associated with the charge injection and improving the reliability of the switches.

#### 4.3. Piezoresistive and other sensors

A wide band gap and its good thermal conductivity and piezoelectric properties make diamond and DLC some of the best materials for sensing applications in harsh environments, involving exposure to high temperature and levels of radiation. They have been utilized for various sensors such as those

detecting temperature [90, 91], gas species or pressure, and UV [92, 93] at temperatures up to 700 °C. Furthermore, as a result of their piezoresistivity, diamond films can be directly used as active sensors themselves [92]. This effect is useful in developing strain gauges, accelerometers and some bio-medical sensors. The piezoresistive gauge factor of diamond films has been found to be in the range of 70–4000 and remains unchanged at high temperatures [94, 95]. Since the elastic modulus of diamond and related materials are in the range of 400–900 GPa, much higher than those of Si and metals, these piezoresistive cantilever sensors can be operated at much high frequencies, as discussed in section 4.1 and have been used to measure partial pressure of oxygen at a temperature of up to 300 °C. A position sensor using polycrystalline diamond was developed for application in cochlear implant probe [94], and various diamond-based gas sensors have been developed for detection of small traces of H<sub>2</sub>, oxygen and CO gases [96–98]. In these applications, the Pt/insulating/semiconductor vertical structure is typically used with a catalyst such as SnO<sub>x</sub> on top of the insulating diamond layer. Adsorption/desorption of gases leads to drastic changes in the current–voltage characteristics. Both mc- and nc-diamond films have been used for gas sensors as the insulating and semiconductor layers and these devices worked up to 500 °C with high sensitivity, repeatability and stability.

Although the piezoresistive effect is generally believed to be only associated with crystalline materials, it has been observed recently in a number of amorphous films such as amorphous Si [99] and amorphous DLC [100, 101]. Piezoresistive gauges with gauge factors of 40–70 have been obtained from hydrogenated amorphous carbon films though the mechanism of the piezoresistive effect is not clear yet. This gauge factor is comparable to, or higher than, the values reported for polycrystalline diamond and polycrystalline silicon. The growth temperature for amorphous DLC (<150 °C) is much lower than that of diamonds (typically at >900 °C). This makes it possible to integrate high temperature DLC piezoresistive sensors with electronic control circuits on the same substrate, thus opening up widespread applications.

Diamond is a semiconducting material with a wide energy band gap (5.5 eV) corresponding to a wavelength of 225 nm so that diamond absorbs only far ultraviolet and vacuum ultraviolet (VUV) radiation. Poly-C has excellent chemical inertness and radiation hardness, high thermal conductivity

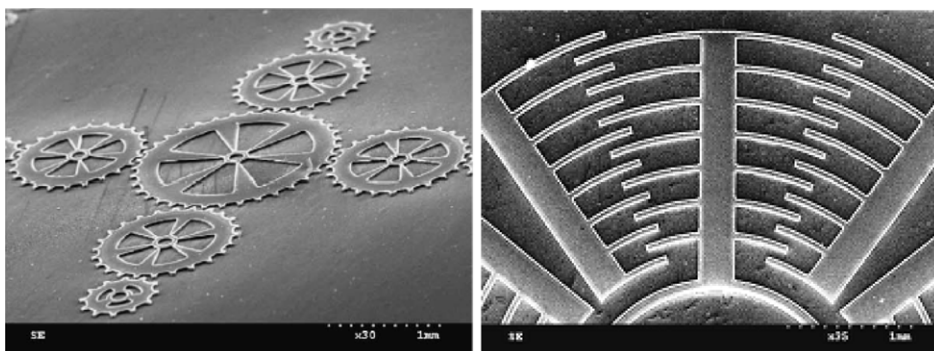


**Figure 16.** Diamond micro-gears and accelerometers ([88], permission to reprint obtained from Elsevier).

and the leakage current of a diamond diode is exceptionally small. It is considered as being solar insensitive and durable to intense VUV radiation with high reliability. This makes it suitable for applications in laser power monitors, for ultraviolet radiation detection in the next generation photolithography, for x-ray source detection as in medical dosimeters and in the high-resolution image sensors used in space exploration [102, 103]. As a result of its high radiation hardness and stability when exposed to high-density radiation, diamond diode-based sensors have also been developed to detect particles in high-energy particle experiments [104, 105]. Since the detection principles are based on the extra carriers generated by UV light and high-energy particles in a pn junction and are very different from those in typical MEMS-based sensors, they will not be discussed here in greater detail.

#### 4.4. Encapsulation

Microsystems often require special packaging when used in real-world environments which may involve direct contact with either chemically corrosive compounds or ambient humidity. Diamond and DLC coatings are one of the best materials for this purpose. Packaging using materials with high thermal conductivity is one way to dissipate heat quickly and so minimize difficulties arising from the generation of local thermal stresses. Diamond and DLC have an excellent thermal conductivity, are chemically inert and are stable up to 600 °C and have found increasing applications in packaging and micro-encapsulation [106–108]. A technology using an all-diamond package for wireless-integrated microsystems with boron-doped diamond as built-in interconnects was developed [106] and demonstrated the ability to achieve an outstanding level of heat dissipation. Resonators using nc-diamond cantilevers were fabricated and encapsulated using the same nc-diamond micro-encapsulation. This type of resonator is suitable for applications in harsh environments and is able to withstand chemical and mechanical attack and high temperatures [108].

#### 4.5. Micro-coolers and heat sinks

Highly integrated electronics are capable of generating heat reaching several hundreds  $W\text{ cm}^{-2}$ , and this rate is exacerbated as the dimensions of the chip shrink. Heat dissipation is an increasingly important challenge for the electronics industry. Miniaturized coolers using a liquid passing through micro-channels represent one of the most advanced technologies used to extract thermal energy from microelectronics circuits such as CPUs. Fluidic capillaries are used as an active cooling mechanism with embedded micro-channels [15, 16]. DLC coatings on Si-based micro-channels can improve the heat capture in these structures because of the high values of near-surface thermal conductivity. A diamond chip can be used as a carrier for heat dissipation of high power electronics devices. Although to date, the majority of DLC-based micro-channels are for use in bio-chemical applications, it is expected that DLC will play a key role in future miniaturization of such micro-cooling systems.

Micro-channels and micro-reactors are two of the basic fluidic components used in biological and chemical applications such as in a ‘lab-on-a-chip’. Although Si

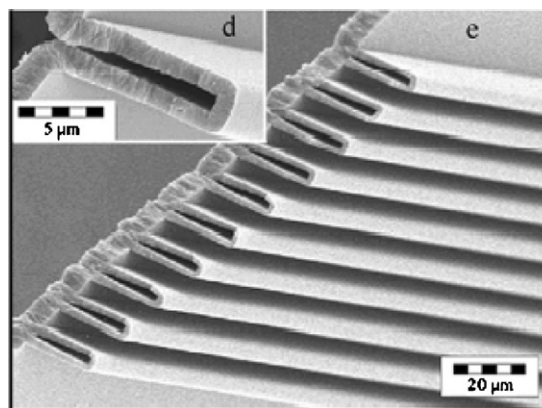


**Figure 17.** SEM cross-section of electroplated diamond micro-channels ([109], courtesy of Dr Zhu, permission to reprint obtained from Elsevier).

and polymers are the dominant materials used in these applications, DLC and diamond possess, in some regard, superior material properties and can be used to both improve performance and broaden applications. DLC is particularly useful in bio-chemical applications and has already been used successfully to fabricate micro-channels [109–111]; figure 17 is one example fabricated from electroplated nc-diamond films. When thick diamond or DLC films are required for micro-fluidic applications, Si moulds made by DRIE can be used. DLC layers are deposited on top of the moulds which are then freed from the Si substrate by a wet etch process. Nanocrystalline diamond films have been used to fabricate freestanding micro-channels, suitable for transportation and analysis of small volumes of chemicals. Micro-reactors with DLC coatings are able to withstand extremes of temperature and many types of chemical reaction without causing cross-contamination or reacting with the analytical chemicals. An integrated microsystem consisting of a micro-chemical reactor chamber, a micro-dosage unit, a bubble jet and a micro-channel has been developed using diamond films in all the critical locations [112]. This microsystem demonstrated superior performance to a Si counterpart in organic, acid and basic solutions with no chemical or mechanical attack, and no evidence of thermal breakdown.

#### 4.6. Micro-mould

The combination of low surface energy, high temperature stability, hydrophobicity and outstanding mechanical properties make diamond thin films excellent materials for use in moulds for nano-imprinting and hot-embossing. Fine structures down to dimensions of a few nanometres have been demonstrated using diamond nano-imprint moulds [113, 114]. Recently, DLC films synthesized by an ion beam on nano-imprint moulds have been investigated, showing superior properties for this application whilst remaining low cost and simple to fabricate [29].

#### 4.7. Field emission tips

Diamond and DLC-based nanostructures can also be used as excellent field emission cathodes in novel applications

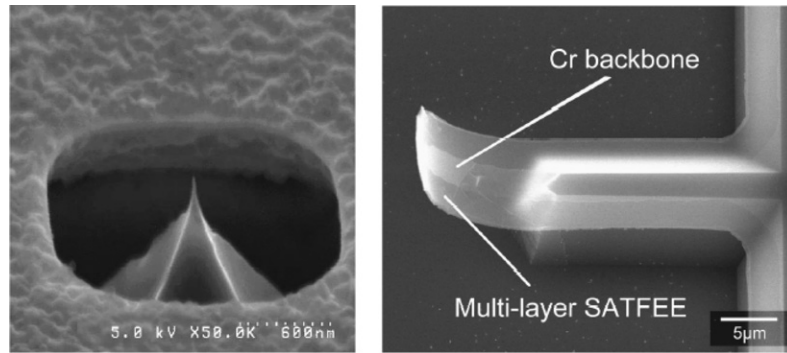


**Figure 18.** Diamond emitter with a self-aligned gated ([118], permission to reprint obtained from Elsevier and the author) and a thin-film field emitter made from a FCVA grown ta-C film [115].

such as sensors, cold cathode and field emission displays because of their low electron affinity and excellent mechanical properties. Various diamond and DLC-based field emitters have been explored in the literature [115–119]. For field emission application, a self-aligned emitter with a controlling gate is the most important issue and technologies have been developed for the preparation of various diamond and DLC emitters. Diamond field emission diodes and triodes with self-aligned gates were made on Si-on-insulator wafers; they showed a high emission current of  $>0.1$  A with a turn-on electrical field of  $3 \text{ V } \mu\text{m}^{-1}$  as shown in figure 18(a) [118]. Figure 18(b) shows a simple self-assembled thin film edge emitter (SATFEE) made from a highly stressed FCVA DLC film on a large Si wafer [115]. The emitters self-assemble once they are released from the substrate by KOH wet etch, forming a good emitter in response to the gradient of stress in the ta-C film. A stable emission with a field enhancement factor up to 80 was obtained.

#### 4.8. Stress-engineered DLC MEMS

Although the large compressive stress in the DLC films is not a desirable material property for most MEMS applications, some novel devices are able to take advantage of the intrinsic stress to form useful structures. The self-assembled field emitter shown in figure 18 is one example. In this section, two stress-engineered MEMS devices, a bi-state microswitch [120] and a normally closed microcage will be introduced [121].

If a double-clamped beam is fabricated from a material with an intrinsic compressive stress, it will buckle once it is released from the substrate: such a beam is illustrated in figure 19. This buckling can be utilized to form a bi-state switch which consists of a bistable beam and the necessary manipulating electrodes. The beam can be switched from one buckled state to another by the application of an electrostatic force via the electrodes. The beam remains fixed in position without requiring an external voltage to hold it. This has potential applications both as a non-volatile memory and in microswitches, micro-relays and micro-tools for punching [120]. The density of a bistable beam-based non-volatile memory is expected to be very high, as the devices are of nanometre size. Similar structures have been proposed for memory application using stressed  $\text{SiN}_x$  membranes [122]. However, DLC layers can have a much higher intrinsic stress

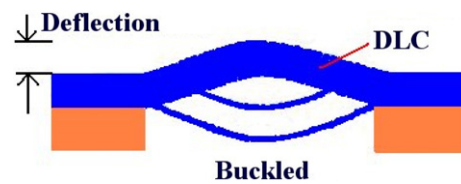


**Figure 19.** Schematic drawing of a bistable beam induced by buckling under the intrinsic compressive stress.

than a  $\text{SiN}_x$  film and it is therefore possible to construct superior bistable beams of small dimension for this application.

When a highly stressed DLC film, grown by FVCA, forms a bilayer structure with a stress-free material, the bilayer will curl once it is released from the substrate. If the DLC film is on the lower side, the bilayer curls upwards: it bends downward if the DLC is on the upper side [85, 121, 123]. By proper design, a fully close microcage can be formed, i.e. by each element of the cage curls by  $180^\circ$ . If a material with a large CTE is used as the upper layer, a compressive thermal stress is generated upon heating the bilayer, which forces the curled bilayer structure to uncurl, i.e. the microcage opens. The opening temperature of the device, i.e. the temperature corresponds to a  $90^\circ$  opening of each finger, is inversely proportional to the difference in CTEs of the two materials [124]. DLC is one of the best materials to be used as the bottom layer of such a microcage, not only because it has a highly compressive intrinsic stress (so encouraging a closed microcage of small diameter), but also because it has a small CTE as discussed in section 4.2, which maximizes the bilayer thermal expansion differential and reduces the opening temperature.

Figure 20(a) shows an SEM of a normally closed SU8/DLC microcage that was fabricated by the authors using a self-aligned two-mask process on a Si substrate. The device consists of a 40 nm ta-C layer and a  $\sim 400$  nm SU8 top layer. An aluminium layer of 40 nm was sandwiched between the DLC and the SU8 to act as a microheater. Electrical tests have shown that the microcages can be open at a temperature approximately  $90^\circ\text{C}$  with a power consumption of only  $\sim 8.0$  mW. Figure 20(b) shows an SEM picture of a microcage with a captured polymer ball, demonstrating its capability to capture a micro-object by confinement rather than by the direct application of a force.



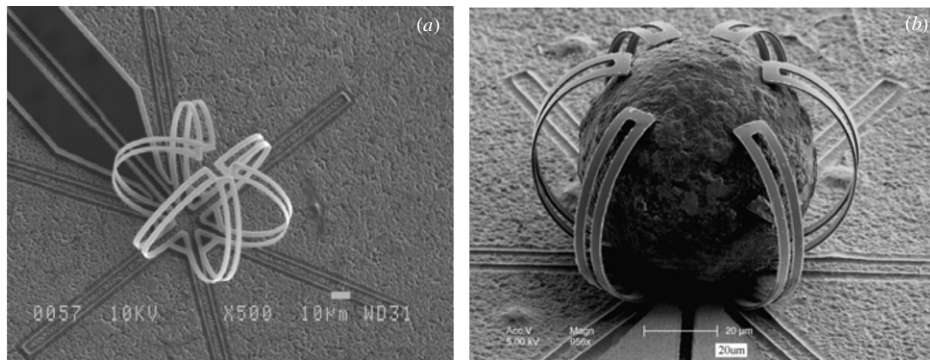


**Figure 20.** SEM picture of (a) an SU8/DLC microcage with a finger length of  $100\ \mu\text{m}$  fabricated by the authors and (b) an SEM picture of the microcage and captured polystyrene micro-ball.

## 5. Conclusions

Diamond and DLC possess a number of material properties which make them particularly attractive for use in MEMS. Their excellent tribological properties can be utilized to improve the stiction, friction and wear resistance of operating MEMS devices. Their high chemical inertness and stability in high temperature environments, together with their biocompatibility and excellent thermal conductivity, can be exploited in the development of biosensors, microfluidic devices for lab-on-a-chip applications, implantable medical devices and miniaturized micro-coolers. The high value of Young's modulus of these materials can be utilized in the design of high frequency resonators. A stress engineering method has been used to develop a unique, normally closed microcage, which has the potential to capture and confine biological cells without the direct application of a force.

## References

- [1] Jacobs-Cook A J 1996 *J. Micromech. Microeng.* **6** 148
- [2] Brown E R 1998 *IEEE Trans. Microw. Theory Technol.* **46** 1868
- [3] Verpoorte E and Rooij N F 2003 *Proc. IEEE* **91** 930
- [4] Tsai N C and Sue C Y 2007 *Sensors Actuators* **136** 178
- [5] Vellekoop M J and Kostner S 2006 *Proc. 20th Eurosensors* vol 1 p 28 (Goteborh, Sweden, September 2006)
- [6] <http://www.sandia.gov/media/NewsRel/NR2000/diamond.htm>
- [7] Spengen W M, Puers R and Wolf I D 2003 *J. Adhes. Sci. Technol.* **17** 563
- [8] Tanner D M, Miller W M, Peterson K A, Dugger M T, Eaton W P, Irwin L W, Senft D C, Smith N F, Tangyunon F P and Miller S L 1999 *Microelectron. Reliab.* **39** 401
- [9] Tanner D M, Walraven J A, Helgesen K S, Irwin L W, Gregory D L, Stake J R and Smith N F 2000 *Proc. IEEE Int. Reliability Phys. Symp. (San Jose, April 2000)* p 139
- [10] Grill A 1997 *Surf. Coat. Technol.* **94–95** 507
- [11] Robertson J 2002 *Mater. Sci. Eng. Rep. R* **37** 129
- [12] Fu Y Q, Yan B B, Loh N L, Sun C Q and Hing P 1999 *J. Mater. Sci.* **34** 2269–83
- [13] Fu Y Q, Loh N L, Yan B B, Sun C Q and Hing P 2000 *Mater. Sci. Eng. A* **282** 38–48
- [14] Fu Y Q, Du H J and Sun C Q 2003 *Thin Solid Films* **424** 107–14
- [15] Bjormen H, Rangsten P and Hjort K 1999 *Sensors Actuators* **73** 24
- [16] Bjormen H, Rangsten P and Hjort K 1999 *Sensors Actuators* **78** 41
- [17] Carlise J A and Auciello O 2003 *Electrochem. Soc. Interface* **12** 28
- [18] Auciello O, Birrell J, Carlise J A, Gerbi J E, Xiao X, Peng B and Espinosa H D 2004 *J. Phys. Condens. Matter* **16** R539
- [19] Kruass A R *et al* 2006 *Diam. Rel. Mater.* **10** 1952
- [20] Friedmann T A and Sullivan J P 2000 *US Patent* 6103305 (August 2000)
- [21] Yang G S, Aslam D M, White M and McGrath J J 1997 *Diam. Rel. Mater.* **6** 394
- [22] Hatta A, Sonada S and Ito T 1999 *Diam. Rel. Mater.* **8** 1470
- [23] Koizumi S, Watanabe K, Hasegawa M and Kanda H 2001 *Science* **292** 1899
- [24] Nesladek M 2005 *Semicond. Sci. technol.* **20** R19
- [25] Gerbi J E, Auciello O, Birrell J, Gruen D M, Alphenaar B W and Carlise J A 2003 *Appl. Phys. Lett.* **83** 2001
- [26] Williams O A, Curant S, Gerbi J E, Gruen D M and Jackman R B 2004 *Appl. Phys. Lett.* **85** 1680
- [27] Zimmermann T, Kubovic M, Denisenko A, Janischowsky K, Williams O A, Gruen D M and Kohn E 2005 *Diam. Rel. Mater.* **14** 416
- [28] Dipalo M, Kustere J, Janischowsky K and Kohn E 2006 *Phys. Status Solidi* **203** 3036
- [29] Meskinis S, Kopustinskas V, Slapikas K, Tamulevicius S, Guobiene A, Gudaitis R and Grigaliunas V 2006 *Thin Solid Films* **515** 636
- [30] Boxman R L, Zhitomirsky V, Alterkop B, Gidalevich E, Beilis I, Keidar M and Goldsmith S 1996 *Surf. Coat. Technol.* **86** 243
- [31] Moseler M, Gumbsch P, Casiraghi C, Ferrari A and Robertson J 2005 *Science* **309** 1545
- [32] Weiler M, Sattel S, Giessen T, Jung K, Ehrhardt H, Veerasamy V S and Robertson J 1996 *Phys. Rev. B* **53** 1594
- [33] Polo M C, Andujar J L, Hary A, Robertson J and Milne W I 2000 *Diam. Rel. Mater.* **9** 663
- [34] Fu Y Q, Luo J K, Flewitt A J, Ong S E, Zhang S and Milne W I 2006 *Appl. Surf. Sci.* **252** 4914
- [35] Kleinsorge B, Ferrari A C, Robertson J and Milne W I 2000 *J. Appl. Phys.* **88** 1149
- [36] Hussain S, Roy R K and Pal A K 2005 *J. Phys. D: Appl. Phys.* **38** 900
- [37] Zhang P, Tay B K and Lau S P 2003 *Diam. Rel. Mater.* **12** 2093
- [38] Zho J P, Chen Z Y, Wang X and Shi T S 2000 *J. Appl. Phys.* **87** 8098
- [39] Chua D H C, Milne W I, Sheeja D, Tay B K and Schneider D 2004 *J. Vac. Sci. Technol. B* **22** 2680
- [40] Zhang S, Bui X L, Fu Y Q and Du H J 2004 *Thin Solid Films* **467** 261
- [41] Zhang S, Sun D, Fu Y Q and Du H J 2003 *Surf. Coat. Technol.* **167** 113
- [42] Williams J A and Le H R 2006 *J. Phys. D: Appl. Phys.* **39** R201

- [43] Kim D, Cao D, Bryant M D, Meng W J and Ling F F 2005 *J. Tribol.* **127** 537
- [44] <http://clifton.mech.northwestern.edu/~me381/project/done/Tribology.pdf>
- [45] Beerschwinger U, Mathieson D, Reuben R L and Yang S J 1994 *J. Micromech. Microeng.* **4** 95
- [46] Smallwood S A, Eapen K C, Patton S T and Zabinski J S 2006 *Wear* **260** 1179
- [47] Liu H W and Bhushan B 2003 *J. Vac. Sci. Technol. A* **21** 1528
- [48] Encke K 1981 *Thin Solids Films* **80** 227
- [49] Voevodin A A, Phelps A W, Zabinski J S and Donley M S 1996 *Diam. Rel. Mater.* **5** 1264
- [50] Voevodin A A, Donley M S and Zabinski J S 1997 *Surf. Coat. Technol.* **92** 42
- [51] Erdemir A, Eyrilmaz O L, Nilufer I B and Fenske G R 2000 *Surf. Coat. Technol.* **133–134** 448
- [52] Le H R, Williams J A and Luo J K 2007 *Int. J. Surf. Sci. Eng.* at press
- [53] Rha J J, Kwon S C, Cho J R, Yim S and Saka N 2005 *Wear* **259** 765
- [54] Scheerder I D et al 2000 *J. Invasive Cardiol.* **12** 389
- [55] Okroj W, Kaminska M, Klimek L, Szymanski W and Walkowiak B 2006 *Diam. Rel. Mater.* **15** 1535
- [56] Grill A 2003 *Diam. Rel. Mater.* **12** 166
- [57] Hauert R 2003 *Diam. Rel. Mater.* **12** 583
- [58] Freitas R A 1999 Foresight Update, 39 Foresight Inst. Palo Alto, CA, USA
- [59] Dearnley P A 1999 *Proc. Inst. Mech. Eng. H* **213** 107
- [60] Khanna P, Villagra A, Kim S, Seto E, Jaroszeski M, Kumar A and Bhansali S 2006 *Diam. Rel. Mater.* **15** 2073
- [61] Yang W, Butler J E, Cai W, Carlisle J, Gruen D, Knickerbocker, Russel J N, Smith L M and Hamers R J 2002 *Nat. Mater.* **1** 253
- [62] Nebel C E, Shin D, Takeuchi D, Yamamoto T, Watanabe H and Nakamura T 2006 *Diam. Rel. Mater.* **15** 1107
- [63] Haertl A, Schmich E, Garrido J A, Hernando J, Catharino S C R, Walter S, Feulner P, Kromka A, Steinmueller D and Stutzmann M 2004 *Nat. Mater.* **3** 736
- [64] Nebel C E, Shin D, Takeuchi D, Yamamoto T, Watanabe H and Nakamura T 2006 *Diam. Rel. Mater.* **15** 1107
- [65] Hamers R J, Butler J E, Lasseter T, Nichols B M, Russell J N, Tse K Y and Yang W S 2005 *Diam. Rel. Mater.* **14** 661
- [66] Higson S P J and Vadgama P M 1995 *Anal. Chim. Acta.* **300** 77
- [67] Carlisle J A 2004 *Nat. Mater.* **3** 668
- [68] Wang J and Carlisle J A 2006 *Diam. Rel. Mater.* **15** 279
- [69] Mahon A R, MacDonald J H, Mainwood A and Ott R J 1999 *Diam. Rel. Mater.* **8** 1748
- [70] Ashby M F 2001 *Materials Selection in Mechanical Design* (Oxford: Butterworth-Heinemann)
- [71] Srikar V T and Spearing S M 2003 *J. Microelectromech. Syst.* **12** 3
- [72] Srikar V T and Spearing S M 2003 *Sensors Actuators A* **102** 279
- [73] Sullivan J P, Friedmann T A, De Boer M P, LaVan D A, Hohlfelder R J, Ashby C I H, Dugger M T, Mitchell M, Dunn R G and Magerkerth A J 2001 *Proc. Mat. Res. Soc. Symp. V* **657** EE7.1
- [74] Ertl S, Adamschik M, Schmid P, Gluche P, Floter A and Kohn E 2000 *Diam. Rel. Mater.* **9** 970
- [75] <http://www.sandia.gov/media/NewsRel/NR2000/diamond.htm>
- [76] Sekaric L, Parpia J M, Craighead H G, Feygelson T, Houston B H and Butler J E 2002 *Appl. Phys. Lett.* **81** 4455
- [77] Mortet V, Haenen K, Potmesil J, Vanecek M and D'Olieslaeger M 2006 *Phys. Status Solidi a* **203** 3158
- [78] Sepulveda N, Aslam D and Sullivan J P 2005 *Diam. Rel. Mater.* **15** 398
- [79] Lamara T, Belmahi M, Elmazria O, Brizoual L, Bougdira J, Remy M and Alnot P 2004 *Diam. Rel. Mater.* **13** 581
- [80] Elmazria O, Benedic F, Ei Hakiki M, Moubchir H, Assouar M B and Silva F 2006 *Diam. Rel. Mater.* **15** 193
- [81] Kim J Y, Chung H J, Kim H J, Cho H M, Yang H K and Park J C 2000 *J. Vac. Sci. Technol. A* **18** 1993
- [82] Zhgoon S, Zhang Q, Yoon S F, Revkov A, Gan B and Rusli A J 2000 *Diam. Rel. Mater.* **9** 1430
- [83] Baltes H, Paul O and Brand O 1998 *Proc. IEEE* **86** 1660
- [84] Hickey R, Kujath M and Hubbard T 2002 *J. Vac. Sci. Technol. A* **23** 971
- [85] Luo J K, He J H, Fu Y Q, Flewitt A J, Fleck N A and Milne W I 2005 *J. Micromech. Microeng.* **15** 1406
- [86] Luo J K, Flewitt A J, Spearing S M, Fleck N A and Milne W I 2005 *J. Micromech. Microeng.* **15** 1527
- [87] Yeatman E M 2005 *J. Micromech. Microeng.* **15** S109
- [88] Fu Y Q, Du H J and Miao J M 2003 *J. Mat. Proc. Technol.* **132** 73
- [89] Chee J L, Karru R, Fisher T S and Peroulis D 2005 *Proc. 13th GAAS Symp. (Paris)*
- [90] Ran J G, Zhang C Q, Ren J and Hong S M 1993 *Diam. Rel. Mater.* **2** 793
- [91] Yang G S, Aslam D M, White M and McGrath J J 1997 *Diam. Rel. Mater.* **6** 394
- [92] Davidson J L, Kang W P, Gurbuz Y, Holmes K C, Davis L G, Wisitorat-a, Kerns D V, Eidson R L and Henerson T 1999 *Diam. Rel. Mater.* **8** 1741
- [93] Ciancaglioni I, Spaziani F, Rossi M C, Conte G, Kononenko V and Ralchenko V 2005 *Diam. Rel. Mater.* **14** 526
- [94] Tang Y X, Aslam D M, Wang J b and Wise K D 2006 *Diam. Rel. Mater.* **15** 199
- [95] Sahli S and Aslam D M 1998 *Sensors Actuators A* **71** 193
- [96] Kang W P and Kim C K 1994 *J. Appl. Phys.* **75** 4237
- [97] Gurbuz Y, Kang W P, Davidson J L and Kerns D V 1998 *Sensors Actuators B* **49** 115
- [98] Gurbuz Y, Kang W P, Davidson J L and Kerns D V 1998 *Diam. Rel. Mater.* **7** 1723
- [99] Alpuim L, Chu V and Conde J P 2002 *IEEE Sensor J.* **2** 336
- [100] Tibrewala A, Peiner E, Bandorf R, Biehl S and Luthje H 2006 *J. Micromech. Microeng.* **16** S75
- [101] Peiner E, Tibrewala A, Bandorf R, Biehl S, Luthje H and Doering L 2006 *Sensors Actuators A* **130–131** 75
- [102] Hayashi K, Tachibana T, Kawakami N, Yokota Y, Kobashi K, Ishihara H, Uchida K, Nippashi K and Matsuoka M 2006 *Diam. Rel. Mater.* **15** 792
- [103] Kaiser A, Kueck D, Benkart P, Munding A, Prinz G M, Heitmann A, Huebner H, Sauer R and Kohn E 2006 *Diam. Rel. Mater.* **15** 1967
- [104] Krammer M et al 2001 *Diam. Rel. Mater.* **10** 1778
- [105] Gorisek A 2006 *Proc. Int. Workshop on Application of Nanocrystalline Diamond and Diamond Like Carbon Material (Calcutta, India, 26 November 2006)* p 163
- [106] Zhu X W, Aslam D M, Tang Y X, Stark B H and Najafi K 2004 *J. Microelectromech. Systems.* **13** 396
- [107] Zhu X W and Aslam D M 2006 *Diam. Rel. Mater.* **15** 254
- [108] Zhu X W, Aslam D M and Sullivan J P 2006 *Diam. Rel. Mater.* **15** 2068
- [109] Guillaudeu S, Zhu X and Aslam D M 2003 *Diam. Rel. Mater.* **12** 65
- [110] Bjorkman H, Rangsten P, Hollman P and Hjort K 1999 *Sensors Actuators A* **73** 24
- [111] Massi M, Ocampo J M, Maciel H S, Grigoro K, Otani C, Santos L V and Mansano R D 2003 *Microelectron. J.* **34** 635
- [112] Adamschik M, Hinz M, Maier C, Schmid P, Seliger H, Hofer E P and Kohn E 2001 *Diam. Rel. Mater.* **10** 722
- [113] Taniguchi J, Takano Y, Miyamoto I, Komuro M and Hiroshima H 2002 *Nanotechnology* **13** 592
- [114] Ohno T, Konoma C, Miyashita H, Kanamori Y and Esashi M 2003 *Japan. J. Appl. Phys.* **42** 3867
- [115] Tsai J T H, Teo K B K and Milne W I 2002 *J. Vac. Sci. Technol. B* **20** 1
- [116] Garguilo J M, Koeck F A M and Nemanich R J 2005 *Phys. Rev. B* **72** 165404

- [117] Yamamoto R, Miyashita K, Hayashi H and Inoue K 2007 *Diam. Rel Mater.* **16** 292
- [118] Kang W P, Davidson J L, Wisitsora-at A, Wong Y M, Takalkar R, Holmes K and Kerms D V 2004 *Diam. Rel. Mater.* **13** 1944
- [119] Geis M W, Twichell J C and Lyszczarz T M 1999 *J. Vac. Sci. Technol. B* **14** 2060
- [120] Guillen F J, Janischowsky K, Kusterer J, Ebert W and Kohn E 2005 *Diam. Rel. Mater.* **14** 411
- [121] Luo J K, Flewitt A J, Fleck N A, Spearing S M and Milne W I 2005 *Appl. Phys. Lett.* **85** 5748
- [122] Tsuchiya Y *et al* 2004 *Proc. Si-Nanoelectronics Workshop* p101
- [123] Vaccaro P O, Kubota K and Aida T 2001 *Appl. Phys. Lett.* **78** 2852
- [124] Luo J K, Huang R, He J H, Fu Y Q, Flewitt A J, Spearing S M, Fleck N A and Milne W I 2006 *Sensors Actuators A* **132** 346